

---

# CAUSAL LEARNING FOR HETEROGENEOUS SUBGROUPS BASED ON NONLINEAR CAUSAL KERNEL CLUSTERING

---

**Lu Liu**

East China University of Science and Technology  
Shanghai, China  
Y30221662@mail.ecust.edu.cn

**Yang Tang**

East China University of Science and Technology  
Shanghai, China  
yangtang@ecust.edu.cn

**Kexuan Zhang**

East China University of Science and Technology  
Shanghai, China  
Y20220069@mail.ecust.edu.cn

**Qiyu Sun**

East China University of Science and Technology  
Shanghai, China  
Y20220069@mail.ecust.edu.cn

## ABSTRACT

Due to the challenge posed by multi-source and heterogeneous data collected from diverse environments, causal relationships among features can exhibit variations influenced by different time spans, regions, or strategies. This diversity makes a single causal model inadequate for accurately representing complex causal relationships in all observational data, a crucial consideration in causal learning. To address this challenge, we introduce the nonlinear Causal Kernel Clustering method designed for heterogeneous subgroup causal learning, illuminating variations in causal relationships across diverse subgroups. It comprises two primary components. First, the construction of a sample mapping function forms the basis of the subsequent nonlinear causal kernel. This function assesses the differences in potential nonlinear causal relationships in various samples, supported by our causal identifiability theory. Second, a nonlinear causal kernel is proposed for clustering heterogeneous subgroups. Experimental results showcase the exceptional performance of our method in accurately identifying heterogeneous subgroups and effectively enhancing causal learning, leading to a great reduction in prediction error.

**Keywords** Causal Learning · Causal Clustering · Heterogeneous Subgroups · Kernel Function

## 1 Introduction

With the problem of multi-source and heterogeneous data in real-world scenarios, identifying causal relationships correctly from observational data becomes an important challenge [1, 2]. However, it is important to acknowledge that various potential factors can affect causal relationships [3, 4, 5, 6]. Therefore, addressing heterogeneous subgroups becomes essential in causal learning [7]. For example, patients may exhibit differing or even opposing responses (effects) to the same treatment (cause), influenced by some potential factors that are unmeasured, such as nutritional and health status [8]. This underscores the importance of categorizing patients into distinct subgroups based on their diverse treatment responses (causal effects) and designing diverse treatment plans. Within each subgroup, the responses of patients to the treatment should be as consistent as possible, whereas significant variances are expected across diverse subgroups.

A variety of methods [9, 10, 11, 12, 13, 14, 15, 16, 17, 18] have been developed for heterogeneous subgroup causal learning, allowing for variations in causal relationships across diverse subgroups. However, the focuses that some methods emphasize are quite different, such as data types [12, 13], specific models [14, 15], and the scenarios of tasks [16, 17]. Moreover, there are also additional conditions [18] imposed on the methods, ensuring the theoretical operability in which the methods operate. These methods perform effectively within their intended contexts, exhibiting impressive accuracy. However, the performances tend to degrade when encountering situations that deviate from the

original, imposing considerable limitations on these methods. As a result of limitations, the scopes of these methods are markedly narrowed, curtailing their abilities to extrapolate and generalize across diverse situations.

Our method adeptly addresses heterogeneous subgroup causal learning by constructing a nonlinear causal kernel and clustering samples with diverse causal relationships. As a flexible causal discovery module, it avoids the need for strong assumptions, such as specific model assumptions or stringent causal conditions. Meanwhile, our method can seamlessly integrate with various causal learning methods, leveraging subgroup information to improve overall performance. The capacity to categorize enhances nuanced and precise comprehension of diversity in causal relationships, effectively addressing the crucial challenge of insufficient representation by a single causal model. This exceptional flexibility extends its applicability, making it suitable for a broad spectrum of scenarios.

The main contributions of this paper are as follows:

- By constructing the sample mapping function, which is central to the nonlinear causal kernel, it maps the samples into a high-dimensional isomorphic to the causal graph space, accompanied by a related causal identifiability theory.
- We propose the nonlinear **C**ausal **K**ernel **C**lustering (CKC) method. It allows us to identify heterogeneous subgroups accurately, revealing variations in causal relationships.
- As a flexible causal discovery module, our method can integrate with established causal learning methods such as ERM [19], KerHRM [20], and Stable Learning [21, 22, 23]. Experimental results demonstrate the exceptional performance of our method in enhancing causal learning.

## 2 Related Work

There is significant attention [24, 25] given to tackling the challenge of heterogeneous subgroup causal learning with distinct focuses. For known heterogeneous subgroups, data fusion is proposed in [26] to extract unique insights from combined data, surpassing the limitations of individual datasets. Meta-learning is introduced in causal inference in [27] to focus on tackling covariate bias by alleviating distributional biases in both training and test data. Furthermore, the method for estimating heterogeneous treatment effects is also proposed in [28] to customize personalized treatments based on insights from diverse subgroups.

However, the identification of heterogeneous subgroups beforehand is frequently impractical in real-world scenarios, as these subgroups typically emerge only through the analysis of observational data. Recognizing the practical constraints that hinder the anticipation of diverse subgroups beforehand, identifying heterogeneous subgroups from observational data becomes a significant challenge, and various methods exist to tackle it. Considering the impact of the temporal dimension on causal relationships, the ACD algorithm in [12] leverages dynamic information sharing for this purpose. Additionally, dual-process intervention learning is proposed in [13] to handle non-stationary time-series data, ensuring the mutual reinforcement of domain indicator recovery and causal structure learning. Some methods exhibit a strong dependence on specific model assumptions. A robust interpretable learning model through additive models is proposed in [14], focusing primarily on variable selection, while the Gaussian model for heterogeneous subgroup causal learning in [15] is limited to binary variables.

## 3 Problem Description

Assuming a set of samples, our focus is on heterogeneous subgroup causal learning [13, 15, 20, 24]. The goal is to causally classify samples, ensuring that within each subgroup, samples exhibit similar nonlinear causal relationships among features. Conversely, causal relationships may vary significantly across diverse subgroups.

Suppose the  $m$  features from  $s$ -th sample, denoted as  $\mathbf{I}^s = [l_1^s, \dots, l_m^s] \in \mathbb{R}^m$ . The values of these features adhere to the causal generation process described by:

$$l_k^s = f_k^s(\text{pa}(k, s)) + e_k^s, \quad (1)$$

for  $k \in \{1, \dots, m\}$ . In (1),  $\text{pa}(k, s)$  represents the direct causal parent features of  $l_k^s$ , influencing  $l_k^s$  casually. The nonlinear term  $f_k^s$  represents the causal relationships between  $\text{pa}(k, s)$  and  $l_k^s$ . The term  $e_k^s$  introduces a non-Gaussian noise component, accounting for some potential unmeasured factors.

Notably, the variation of causal relationships between subgroups is significantly larger than within subgroups, leading to the following definition of subgroup invariance.

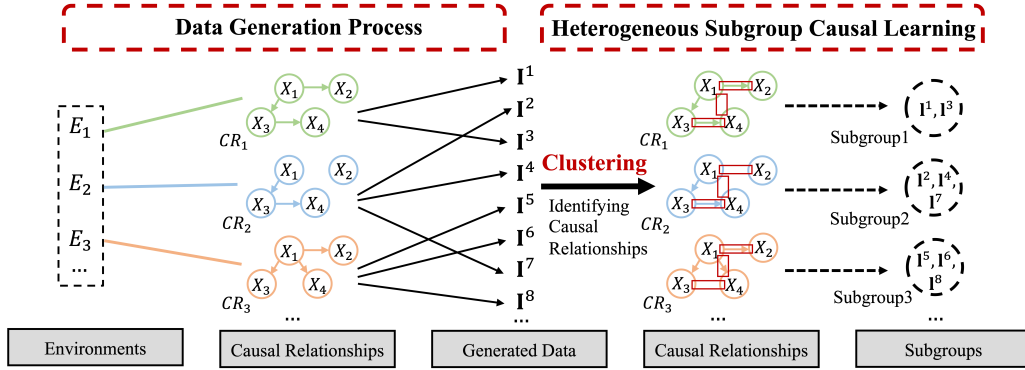


Figure 1: An illustration of the process of generating multi-source and heterogeneous data from various environments and our approach to heterogeneous subgroup causal learning, taking four features ( $m = 4$ ) as an example.  $E_1, \dots$  denote the multiple environments,  $X_1, \dots$  denote the features,  $CR_1, \dots$  denote the diverse causal relationships between features, and  $I^s (s \in \{1, 2, \dots\})$  denote the data generated by the corresponding causal relationships. Our objective is to obtain heterogeneous subgroups through clustering, identifying various causal relationships.

**Definition 3.1 (Subgroup Invariance)** For any feature  $X_k, k \in \{1, \dots, m\}$  and the subgroups of samples  $G = \{g_1, \dots, g_r\}$ , there exists subgroup invariance regarding the causal relationships, which corresponds to (1):

$$X_k = f_k^{g_i}(pa(k, g_i)) + e_k^{g_i}. \quad (2)$$

Drawing from Definition 3.1, we introduce the nonlinear CKC method. This method aims at clustering samples with similar nonlinear causal relationships and identifying heterogeneous subgroups, thereby revealing variations in causal relationships across different subgroups [15, 20].

## 4 Method

Numerous studies have deeply explored the field of heterogeneous subgroup causal learning [11, 13, 15, 29, 20, 24]. [20] employs kernelized heterogeneous risk minimization, which cleverly achieves the dual objectives of heterogeneous subgroup exploration and causal invariant learning in the kernel space, offering a new insight for nonlinear scenarios. In terms of heterogeneous subgroup exploration, it constructs a kernel clustering algorithm based on the sample mapping function, enabling precise capture of heterogeneous subgroup information, which is crucial for causal invariant learning. Inspired by [20], we propose a kernel clustering method based on the sample mapping function to capture heterogeneous subgroup information. On one hand, the sample mapping function captures nonlinear relationship within the samples. On the other hand, clustering operation facilitates the in-depth extraction of heterogeneous subgroup causal information. By capturing the heterogeneous subgroup information, we could utilize the subgroup information as causal signal warning and stable feature mining, enhancing the effectiveness and reliability of subsequent causal learning methods.

To ensure that our sample mapping function can fully capture heterogeneous subgroup information, it is essential to consider both the dependence and independence between features during the construction process [2, 17, 18, 30, 31]. This statistical approach leads to the proposal of our binary decision method based on dependence/independence, which is central to our design idea. In statistics, the dependence between pairs of features is commonly measured using correlation coefficients [32, 33, 34, 35], while independence is often verified using the chi-square test [36, 37]. Thus, on one hand, we design a correlation coefficient statistic to accurately assess the dependencies between feature pairs [33, 34, 35, 38, 39, 40]; On the other hand, we use the common chi-square statistic to scientifically test feature independence [36, 37, 41]. By comparing dependence [35, 33] and independence [36, 37, 41], we construct our sample mapping function through the design idea of binary decision, that comprehensively represents the relationships within the data, facilitating the capture of complex patterns.

Our method introduces a sample mapping function that centers on the samples, mapping them into a high-dimensional space. Subsequently, this mapping is utilized to construct a corresponding nonlinear causal kernel, of extreme importance for clustering [20].

#### 4.1 Marginal Distance Covariance

This section focuses on developing a metric to measure the dependence between features. In statistics, correlation coefficients are commonly used to describe linear dependence between features [32, 42, 29, 43, 44, 45]. However, for nonlinear dependence, more complex statistics are required, such as distance correlation coefficients [33, 34, 35, 46, 29, 38, 39, 40]. [35] proposes the use of a  $u$ -centered version [46, 38] of distance matrix to construct an extended form of the concept of distance covariance. Through eliminating sample bias, [35] results in a standardized coefficient for evaluating nonlinear dependence between features. Inspired by [33, 35, 46, 38], we introduce the concept of marginal distance covariance based on the  $u$ -centered version of distance matrix.

**Notation.** In this paper, both  $n$  and  $n'$  represent the number of samples,  $m$  represents the number of features. For any  $d$ -dimensional square matrix  $\mathbf{M} = (m_{st})_{s,t=1}^d \in \mathbb{R}^{d \times d}$ ,  $\tilde{\mathbf{M}} = (\tilde{m}_{st})_{s,t=1}^d \in \mathbb{R}^{d \times d}$  is used to represent the  $u$ -centered version [35] of matrix  $\mathbf{M}$ , where  $\tilde{m}_{st} = m_{st} - \frac{1}{d-2} \sum_{u=1}^d m_{ut} - \frac{1}{d-2} \sum_{v=1}^d m_{sv} + \frac{1}{(d-1)(d-2)} \sum_{u,v=1}^d m_{uv}$ . For any matrix  $\mathbf{N} \in \mathbb{R}^{d_1 \times d_2}$ , let  $\mathbf{N}_i$  and  $\mathbf{N}_j$  represent the  $i$ -th row and the  $j$ -th column in  $\mathbf{N}$ , respectively.

**Lemma 4.1 (Sample Distance Matrix [33, 34, 35, 29, 46, 38])** For samples  $\mathcal{S} = [X_1, \dots, X_m] \in \mathbb{R}^{n \times m}$ , the sample distance matrix is denoted as  $\mathbf{H} \in \mathbb{R}^{n \times n \times m}$ , with  $\mathbf{H}_{i,i',j} = |\mathcal{S}_{i,j} - \mathcal{S}_{i',j}|$ .  $\mathbf{H}_{\cdot,\cdot,j}$  denotes the sample distance matrix for feature  $X_j$ .

[35] employs the  $u$ -centered version to design the partial distance covariance for ternary features. Since our study focuses on the causal relationships between all pairs of features, we design the marginal distance covariance by using the  $u$ -centered version [33, 35, 46, 38], allowing for a more appropriate evaluation of the dependence between pairs of features.

**Definition 4.1 (Marginal Distance Covariance [33, 35, 46, 38])** For two features  $X_p$  and  $X_q$ , with their sample distance matrices  $\mathbf{H}_{\cdot,\cdot,p} = [\mathcal{P}_1, \dots, \mathcal{P}_n]$  and  $\mathbf{H}_{\cdot,\cdot,q} = [\mathcal{Q}_1, \dots, \mathcal{Q}_n]$ , the marginal distance covariance between the features is defined as:

$$mdCov^2(X_p, X_q) = \sum_{\alpha=1}^n \sum_{\beta=1}^n dCov^2(\mathcal{P}_\alpha, \mathcal{Q}_\beta), \quad (3)$$

$$dCov^2(\mathcal{P}_\alpha, \mathcal{Q}_\beta) = \int_{\mathbb{R}^{2n}} \frac{|\phi_{\mathcal{P}_\alpha, \mathcal{Q}_\beta}(\delta, \rho) - \phi_{\mathcal{P}_\alpha}(\delta)\phi_{\mathcal{Q}_\beta}(\rho)|^2}{c|\delta|^{n+1}|\rho|^{n+1}} d\delta d\rho, \quad (4)$$

where  $\mathcal{P}_\alpha, \mathcal{Q}_\beta$  represent the corresponding low-dimensional components of the sample distance matrices  $\mathbf{H}_{\cdot,\cdot,p}$  and  $\mathbf{H}_{\cdot,\cdot,q}$ ,  $c = \pi^{n+1}/\tau^2(\frac{n+1}{2})$ ,  $|\cdot|$  represents the Euclidean norm defined as  $|x| = \sqrt{\bar{x}^T x}$  for and vector  $x$  ( $\bar{x}$  represents the conjugate of  $x$ ),  $\phi_{\mathcal{P}_\alpha}$  and  $\phi_{\mathcal{Q}_\beta}$  are the characteristic functions of  $\mathcal{P}_\alpha$  and  $\mathcal{Q}_\beta$  respectively,  $\phi_{\mathcal{P}_\alpha, \mathcal{Q}_\beta}$  is the joint characteristic function. The alternative simplified form of  $dCov^2(\mathcal{P}_\alpha, \mathcal{Q}_\beta)$  is given as:

$$dCov^2(\mathcal{P}_\alpha, \mathcal{Q}_\beta) = \langle \tilde{\mathbf{A}}_\alpha, \tilde{\mathbf{B}}_\beta \rangle, \quad (5)$$

where  $\mathbf{A}_\alpha, \mathbf{B}_\beta$  represent the sample distance matrices generated from  $\mathcal{P}_\alpha, \mathcal{Q}_\beta$ , and  $\tilde{\mathbf{A}}_\alpha, \tilde{\mathbf{B}}_\beta$  represent the  $u$ -centered versions of  $\mathbf{A}_\alpha, \mathbf{B}_\beta$ .

By eliminating sample bias [35] from the marginal distance covariance, we can obtain the corresponding marginal distance correlation coefficient, which serves as a metric to evaluate the nonlinear dependence between two features [33, 35].

$$mdCor^2(X_p, X_q) = \frac{mdCov^2(X_p, X_q)}{\sqrt{mdCov^2(X_p, X_p)} \cdot \sqrt{mdCov^2(X_q, X_q)}}. \quad (6)$$

*Remark.* Current methods [32, 33, 47, 48, 49] predominantly focus on quantifying linear causal relationships. Addressing this limitation, the marginal distance covariance is introduced as a metric for capturing nonlinear causal relationships.

## 4.2 Sample Mapping Function Based on Hypothesis Testing

In this section, we will explore the construction of metric for determining the independence between pairs of features [4] and design sample mapping function that can reflect the corresponding causal relationships between features. As is well known, the chi-squared statistic is widely used for testing the independence of features [36, 37]. For instance, in medical research, chi-squared test can be used to examine whether a particular disease is independent of different lifestyle factors such as smoking or drinking. In market research, it can be used to analyze whether consumers preference for different brands are independent of factors such as gender or age. Thus, we propose the hypothesis framework [33, 34, 36, 37] for independence testing and use the chi-squared statistic as an indicator to assess the independence between features.

**Lemma 4.2 (Hypothesis Testing [33, 34, 36, 37])** *The hypothesis testing is given to ascertain the independence of two features:*

$$H_0 = \{(X_p, X_q) | X_p \perp\!\!\!\perp X_q\}, \quad (7)$$

$$H_1 = \{(X_p, X_q) | X_p \not\perp\!\!\!\perp X_q\}. \quad (8)$$

*If the condition  $H_0$  holds,  $X_p$  and  $X_q$  are independent. Conversely, if the condition  $H_1$  holds, there exists nonlinear dependence between the two features.*

Expanding upon Lemma 4.2, we define the sample mapping function, utilizing marginal distance covariance to gauge the similarities among samples. Specifically, we first design the marginal distance covariance through Definition 4.1. After removing the sample bias, it can be used to measure the dependence between features [33, 35]. Meanwhile, utilizing the independence hypothesis test from Lemma 4.2, we use the common chi-squared statistics [36, 37] to assess the independence between features. By leveraging the disparity between these two statistics, the sample mapping function could assessment both dependence and independence between features, revealing the causal relationships behind them comprehensively.

**Definition 4.2 (Sample Mapping Function [20, 33, 34, 35])** *For samples  $S \in \mathbb{R}^{n \times m}$ , consider the sample distance matrix  $\mathbf{H} \in \mathbb{R}^{n \times n \times m}$ , and its  $u$ -centered processed normalized matrix  $\mathbf{Z} \in \mathbb{R}^{n \times n \times m}$ ,  $\mathbf{Z}_{i,i',j} = \frac{C_{i,i',j}}{\bar{\mathbf{H}}_{i,i',j}}$ , where  $C_{i,i',j}$  is the  $u$ -centered version of  $\mathbf{H}_{i,i',j}$  and  $\bar{\mathbf{H}}_{i,i',j}$  is the mean over  $\mathbf{H}_{i,i',j}$ . Define the sample mapping function  $\Phi(S_i): \mathbb{R}^m \rightarrow \mathbb{R}^{m \times m}$  as:*

$$\Phi(S_i) = \sum_{\alpha=1}^n \sum_{\beta=1}^n \sum_{\zeta=1}^n V_{\zeta,\alpha} \cdot V_{\zeta,\beta}^T - \Gamma(\nu), \quad (9)$$

$$V_{\zeta,\gamma} = \text{Vec}(|\mathbf{Z}_{\zeta,\gamma,\cdot} - \mathbf{Z}_{i,\gamma,\cdot}|), \forall \gamma \in \{\alpha, \beta\}, \quad (10)$$

$$\Gamma(\nu)_{j,j'} = \begin{cases} n\chi_{1-\nu}^2(1), & j \neq j' \\ 0, & j = j' \end{cases}, \quad (11)$$

*for  $i \in \{1, 2, \dots, n\}$ , where  $|\cdot|$  represents the absolute value,  $\text{Vec}$  represents the column vector form,  $\Gamma(\nu) \in \mathbb{R}^{m \times m}$ ,  $\nu$  represents the significance level, and  $\chi_{1-\nu}^2(1)$  represents the chi-square value with 1 degree of freedom.*

*Proof.* The first term of Definition 4.2 represents the form of marginal distance covariance after eliminating bias:  $\sum_{\alpha=1}^n \sum_{\beta=1}^n \sum_{\zeta=1}^n V_{\zeta,\alpha} \cdot V_{\zeta,\beta}^T$ , which is the marginal distance correlation coefficient that can evaluate feature dependence [33, 35]. Compared to the conventional distance correlation coefficient [4, 32], it incorporates an extra layer of summation operation. This results in an  $n$ -fold amplification of the second term chi-squared statistic  $n\chi_{1-\nu}^2(1)$  with the degree of freedom for a single sample being 1 to ensure the accuracy of the result [41, 50, 51]. From the perspective of our sample mapping function  $\Phi(S_i)$ , the element in the  $p$ -th row and  $q$ -th column represents the disparity between the marginal distance correlation coefficient statistic and the chi-squared statistic for features  $X_p$  and  $X_q$ . If the element is greater than 0, it indicates that the non-linear dependence of features reflected by the marginal distance correlation coefficient statistic is more significant than the independence of features reflected by the chi-square statistic:  $(\sum_{\alpha=1}^n \sum_{\beta=1}^n \sum_{\zeta=1}^n V_{\zeta,\alpha} \cdot V_{\zeta,\beta}^T)_{p,q} > (n\chi_{1-\nu}^2(1))_{p,q}$ , i.e.,  $(\sum_{\alpha=1}^n \sum_{\beta=1}^n \sum_{\zeta=1}^n V_{\zeta,\alpha} \cdot V_{\zeta,\beta}^T)_{p,q} - (n\chi_{1-\nu}^2(1))_{p,q} > 0$ . It suggests a stronger nonlinear dependence between features. Conversely, if the element is less than 0:  $(\sum_{\alpha=1}^n \sum_{\beta=1}^n \sum_{\zeta=1}^n V_{\zeta,\alpha} \cdot V_{\zeta,\beta}^T)_{p,q} \leq (n\chi_{1-\nu}^2(1))_{p,q}$ , i.e.,  $(\sum_{\alpha=1}^n \sum_{\beta=1}^n \sum_{\zeta=1}^n V_{\zeta,\alpha} \cdot V_{\zeta,\beta}^T)_{p,q} - (n\chi_{1-\nu}^2(1))_{p,q} \leq 0$ , the features are more in line with the independence. This method enables us to explore both dependence and independence between features through a binary decision method, allowing for a more nuanced and comprehensive understanding of the causal relationships between features.

*Remark.* Differing from the conventional emphasis on causal relationships between features, the sample mapping function shifts the focus to the samples themselves.

**Theorem 4.1** For a significance level  $\nu$ , concerning features  $X_p$  and  $X_q$ , if the condition  $\sum_{i=1}^n \Phi(\mathbf{S}_{i,})_{p,q} > 0$  holds, it implies that the features are not independent i.e.,  $X_p \not\perp X_q$ , indicating the presence of nonlinear dependence. Conversely, if the condition  $\sum_{i=1}^n \Phi(\mathbf{S}_{i,})_{p,q} \leq 0$  holds, it implies that the features are independent i.e.,  $X_p \perp X_q$ .

*Proof.* As is shown above, for features  $X_p$  and  $X_q$ , if  $(\sum_{\alpha=1}^n \sum_{\beta=1}^n \sum_{\zeta=1}^n V_{\zeta,\alpha} \cdot V_{\zeta,\beta}^T)_{p,q} > (n\chi_{1-\nu}^2(1))_{p,q}$ , i.e.,  $(\sum_{\alpha=1}^n \sum_{\beta=1}^n \sum_{\zeta=1}^n V_{\zeta,\alpha} \cdot V_{\zeta,\beta}^T)_{p,q} - (n\chi_{1-\nu}^2(1))_{p,q} > 0$ , it indicates that the degree of nonlinear dependence between features is more significant than the degree of feature independence. Therefore, we conclude that:  $X_p \not\perp X_q$ . Conversely, if  $(\sum_{\alpha=1}^n \sum_{\beta=1}^n \sum_{\zeta=1}^n V_{\zeta,\alpha} \cdot V_{\zeta,\beta}^T)_{p,q} \leq (n\chi_{1-\nu}^2(1))_{p,q}$ , i.e.,  $(\sum_{\alpha=1}^n \sum_{\beta=1}^n \sum_{\zeta=1}^n V_{\zeta,\alpha} \cdot V_{\zeta,\beta}^T)_{p,q} - (n\chi_{1-\nu}^2(1))_{p,q} \leq 0$ , it indicates that the features are more in line with the independence. Therefore, we conclude that:  $X_p \perp X_q$ . Meanwhile, considering the potential presence of outliers in multi-source and heterogeneous data, [32] emphasizes that these outliers can lead to incorrect final decisions. Thus, we use a summation form to make the final binary decision:  $\sum_{i=1}^n \Phi(\mathbf{S}_{i,})_{p,q} > 0$  for  $X_p \not\perp X_q$ , and  $\sum_{i=1}^n \Phi(\mathbf{S}_{i,})_{p,q} \leq 0$  for  $X_p \perp X_q$ .

The subsequent section explores the causal identifiability theory of the sample mapping function  $\Phi(\mathbf{S}_{i,})$ , providing support for Theorem 4.1 and the clustering.

### 4.3 Nonlinear Causal Kernel

Given our primary use of mapping to assess sample similarity rather than directly inferring causal relationships between features, the corresponding nonlinear causal kernel is constructed for the sample mapping function [20, 52, 29, 53].

Inspired by [20], we construct our nonlinear causal kernel to measure the similarity of samples in the mapping space, ensuring the clustering more accurately. [35] defines a cosine-similarity measure to assess similarity of samples in the mapped space, with a combination of inner products and norms. [10, 54, 55, 56, 57] propose Frobenius inner-product and norm for theoretical design in causal learning. Building upon these methods [10, 20, 35, 54, 55, 56, 57], we design our nonlinear causal kernel for our sample mapping function through cosine-similarity from and Frobenius inner-product norm combinations, providing an approximate formula from the perspective of inner-product for subsequent proof.

**Definition 4.3 (Nonlinear Causal Kernel [10, 20, 35, 54, 29])** Integrating the sample mapping function  $\Phi(\mathbf{S}_{i,})$ , the Frobenius inner product  $\langle \cdot, \cdot \rangle_F$ , and its norm  $\|\cdot\|_F$ , we define the nonlinear causal kernel  $\kappa(\mathbf{S}_{i,}, \mathbf{S}_{i',})$  between two samples as:

$$\kappa(\mathbf{S}_{i,}, \mathbf{S}_{i',}) = \frac{\langle \Phi(\mathbf{S}_{i,}), \Phi(\mathbf{S}_{i',}) \rangle_F}{\|\Phi(\mathbf{S}_{i,})\|_F \cdot \|\Phi(\mathbf{S}_{i',})\|_F}. \quad (12)$$

The nonlinear causal kernel can be approximated by the formula:  $\kappa(\mathbf{S}_{i,}, \mathbf{S}_{i',}) \propto \sum_{j=1}^m \sum_{j'=1}^m \Phi(\mathbf{S}_{i,})_{j,j'} \cdot \Phi(\mathbf{S}_{i',})_{j,j'}$ .

*Proof.* The nonlinear causal kernel is constructed through:  $\kappa(\mathbf{S}_{i,}, \mathbf{S}_{i',}) \approx \cos(\theta) = \frac{\langle A, B \rangle}{|A| \cdot |B|} = \frac{\langle A, B \rangle}{\sqrt{\langle A, A \rangle} \cdot \sqrt{\langle B, B \rangle}} = \frac{\langle \Phi(\mathbf{S}_{i,}), \Phi(\mathbf{S}_{i',}) \rangle_F}{\sqrt{\langle \Phi(\mathbf{S}_{i,}), \Phi(\mathbf{S}_{i,}) \rangle_F} \cdot \sqrt{\langle \Phi(\mathbf{S}_{i',}), \Phi(\mathbf{S}_{i',}) \rangle_F}} = \frac{\langle \Phi(\mathbf{S}_{i,}), \Phi(\mathbf{S}_{i',}) \rangle_F}{\|\Phi(\mathbf{S}_{i,})\|_F \cdot \|\Phi(\mathbf{S}_{i',})\|_F} \propto \langle \Phi(\mathbf{S}_{i,}), \Phi(\mathbf{S}_{i',}) \rangle_F = \sum_{j=1}^m \sum_{j'=1}^m \Phi(\mathbf{S}_{i,})_{j,j'} \cdot \Phi(\mathbf{S}_{i',})_{j,j'}$ . Due to the high-dimensional features in the new space resulting from our mapping function, the computations become increasingly difficult as the dimensionality grows. To address this, we have adopted the Frobenius form for matrix construction, which is well-known for its efficiency in handling large-scale data calculations [58, 59, 60, 61, 62].

We will delve into the kernel clustering method based on our sample mapping function, leveraging Theorem 4.2 to prove that our method could unearth heterogeneous subgroup causal information, consequently enhancing the performance of subsequent causal learning methods.

**Theorem 4.2** Consider two sample sets  $\mathbf{S} \in \mathbb{R}^{n \times m}$  and  $\mathbf{S}' \in \mathbb{R}^{n' \times m}$  with the same features  $X = (X_1, \dots, X_m)$ . If the condition  $\sum_{i=1}^n \sum_{i'=1}^{n'} \kappa(\mathbf{S}_{i,}, \mathbf{S}'_{i',}) < 0$  holds, it indicates the presence of distinct nonlinear causal relationships between the two sample sets.

*Proof.* Based on Definition 4.3 and the approximate formula, if the condition  $\sum_{i=1}^n \sum_{i'=1}^{n'} \kappa(\mathbf{S}_{i,}, \mathbf{S}'_{i',}) < 0$  holds, it is evident that at least one pair of features exists, denoted as  $(j, j') \in \{1, \dots, m\}$ , where  $\Phi(\mathbf{S}_{i,})_{j,j'}$  and  $\Phi(\mathbf{S}'_{i',})_{j,j'}$  exhibit opposite signs. Assume  $\Phi(\mathbf{S}_{i,})_{j,j'} > 0$  and  $\Phi(\mathbf{S}'_{i',})_{j,j'} < 0$ . According to Theorem 4.1, it can be proved that  $X_j \not\perp X_{j'}$  in samples  $\mathbf{S}$ , but  $X_j \perp X_{j'}$  in samples  $\mathbf{S}'$ . It implies that there exists different nonlinear causal relationships underpinning two sample sets  $\mathbf{S}$  and  $\mathbf{S}'$ .

*Remark.* Drawing on Definition 4.3 and Theorem 4.1, the direction of elements in our sample mapping function  $\Phi(\mathbf{S}_{i,})$  can uncover varying causal relationships among features. Theorem 5.1 proves that the nonlinear causal kernel, which is

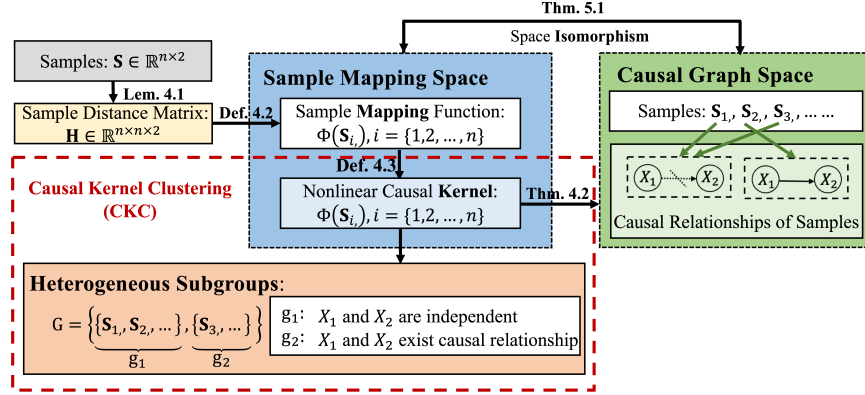


Figure 2: The operated framework of our method (CKC) which is based on samples  $\mathbf{S} \in \mathbb{R}^{n \times 2}$  with two features ( $m = 2$ ).

built upon our sample mapping function, is capable of discerning different causal relationships between features. This capability allows our method to extract heterogeneous subgroup causal information, thus enhancing the performance of subsequent causal learning methods.

Based on the theoretical framework presented earlier, we propose the nonlinear CKC method, as depicted in Fig. 2 with illustration employing two features  $X_1$  and  $X_2$  ( $m = 2$ ). For samples  $\mathbf{S} \in \mathbb{R}^{n \times 2}$ , the distance matrix  $\mathbf{H} \in \mathbb{R}^{n \times n \times 2}$  is initially constructed. Subsequently, our sample mapping function  $\Phi(\mathbf{S}_i)$  is employed to map the samples to a high-dimensional space, and the kernel function  $\kappa(\mathbf{S}_i, \mathbf{S}_{i'})$  is then constructed, where  $i, i' \in \{1, 2, \dots, n\}$ . In the subsequent section, we establish theoretically that the sample mapping space is isomorphic to the causal graph space, ensuring that the subgroups identified by our method are causally heterogeneous. As shown in Fig. 2, a notable example illustrates the absence of causal relationship between features in both samples  $\mathbf{S}_1$  and  $\mathbf{S}_3$ , while such a causal relationship exists in sample  $\mathbf{S}_2$ . Considering the different causal relationships between features, the samples  $\mathbf{S}_1$  and  $\mathbf{S}_3$  are more likely clustered into one subgroup.

## 5 Causal Identifiability Theory

### 5.1 Space Isomorphism

To demonstrate that our method can identify heterogeneous subgroups and be effectively applied in the causal learning methods, we need to consider from two aspects. On one hand, we need to ensure the rationality of the constructed mapping function, indicating that the operation in the mapping space are consistent with those in the original sample space. On the other hand, we need to explore the causal identifiability of our sample mapping function through mapping space, ensuring that our method could reveal and quantify the causal relationships directly.

Initially, it is necessary to demonstrate that the sample mapping function  $\Phi(\mathbf{S}_i)$  is bijective, indicating isomorphism between the original sample space  $\mathbb{R}^m$  and the mapping space  $\mathbb{R}^{m \times m}$  with a property of distance invariance [63, 64].

The bijective property of a mapping function is frequently utilized to establish an isomorphism between the mapping space and the original space in mathematics, ensuring that the mapping space and the original space share the same properties [63, 64]. Therefore, To ensure the rationality and effectiveness of using the mapping space instead of the original space for our subsequent clustering operation, it is necessary to prove the bijective property of our sample mapping function firstly. Based on the commonly used approach for proving bijective property in the field of mathematics through injective property and surjective property, we prove our sample mapping function by separately proving these two properties [65, 66].

*Proof.* Consider any mapping function  $\Phi(\mathbf{S}_i) \in \mathbb{R}^{m \times m}$  and  $\Phi(\mathbf{S}_{i'}) \in \mathbb{R}^{m \times m}$ , if the condition  $\Phi(\mathbf{S}_i) = \Phi(\mathbf{S}_{i'})$  holds, it implies that  $\mathbf{Z}_{i,\cdot} = \mathbf{Z}_{i',\cdot}$  as well as  $\mathbf{S}_i = \mathbf{S}_{i'}$ , where  $\mathbf{S}_i \in \mathbb{R}^m$  and  $\mathbf{S}_{i'} \in \mathbb{R}^m$ . This ensures that the sample mapping function  $\Phi(\mathbf{S}_i) : \mathbb{R}^m \rightarrow \mathbb{R}^{m \times m}$  is injective; Furthermore, the mapping space  $\mathbb{R}^{m \times m}$  is comprised of the sample mapping function  $\Phi(\mathbf{S}_i)$ . For each element  $\eta \in \mathbb{R}^{m \times m}$ , there exists a sample  $\mathbf{S}_\epsilon$ , such that  $\Phi(\mathbf{S}_\epsilon) = \eta$ , confirming that the sample mapping function  $\Phi(\mathbf{S}_i) : \mathbb{R}^m \rightarrow \mathbb{R}^{m \times m}$  is surjection.

## 5.2 Causal Identifiability

This section demonstrates the causal identifiability of our developed sample mapping function  $\Phi(\mathbf{S}_{i,\cdot})$ .

To demonstrate that our method can identify heterogeneous subgroups and be effectively applied in the causal learning methods, we need to explore the causal identifiability of our sample mapping function in mapping space, showing the relationship between the mapping space and causal graph space. It is common in mathematics to establish theoretical analyses by defining two spaces and proving their relationships [63, 67]. Therefore, we need first define the concept of two spaces. Inspired by [7, 68, 69, 70, 71], we consider to design the concept of equivalent causal graph with certain conditions, further demonstrating that our mapping function can reflect causal meanings. To this end, we introduce a new concept of  $m$ -connectivity:  $N^{\mathcal{G}'}$ .

**Definition 5.1 (Causal Graph Space [7, 68, 69, 70])** Consider a causal graph  $\mathcal{G} = (O^{\mathcal{G}}, E^{\mathcal{G}})$ , where  $O^{\mathcal{G}}$  represents the nodes of the causal graph  $\mathcal{G}$ , and  $E^{\mathcal{G}}$  represents the edges of the causal graph  $\mathcal{G}$ .  $N^{\mathcal{G}}$  represents the pairs of nodes  $(j, j')$  with  $m$ -connectivity, indicating that the longest path between the nodes is  $m$ . For two causal graphs  $\mathcal{G} = (O^{\mathcal{G}}, E^{\mathcal{G}})$  and  $\mathcal{G}' = (O^{\mathcal{G}'}, E^{\mathcal{G}'})$  with  $O^{\mathcal{G}} = O^{\mathcal{G}'}$ , they are equivalent if and only if  $N^{\mathcal{G}} = N^{\mathcal{G}'}$ . We use  $\mathbb{G}^m$  to represent the space of equivalent causal graphs.

We provide a simple example and mathematical proof to illustrate the rationality of Definition 5.1.

*Proof.* Since the longest path of a node does not exceed the total number of nodes in the causal graph, for two causal graphs  $\mathcal{G} = (O^{\mathcal{G}}, E^{\mathcal{G}})$  and  $\mathcal{G}' = (O^{\mathcal{G}'}, E^{\mathcal{G}'})$  with same four nodes:  $O^{\mathcal{G}} = O^{\mathcal{G}'} = \{O_1, O_2, O_3, O_4\}$ ,  $m$  only makes sense when taking 1, 2, or 3. Assume that causal graph  $\mathcal{G}$  is:  $E^{\mathcal{G}} = O_2 - O_1 - O_3 - O_4$ , and causal graph  $\mathcal{G}'$  is:  $E^{\mathcal{G}'} = O_1 - O_2 - O_4 - O_3$ , having different causal relationships. The  $m$ -connectivity set of causal graph  $\mathcal{G}$  is:

$$N^{\mathcal{G}} = \begin{cases} \{(O_1, O_2), (O_1, O_3), (O_3, O_4)\}, & m = 1 \\ \{(O_1, O_4), (O_2, O_3)\}, & m = 2 \\ \{(O_2, O_4)\}, & m = 3. \end{cases}$$

The  $m$ -connectivity set of causal graph  $\mathcal{G}'$  is:

$$N^{\mathcal{G}'} = \begin{cases} \{(O_1, O_2), (O_2, O_4), (O_3, O_4)\}, & m = 1 \\ \{(O_1, O_4), (O_2, O_3)\}, & m = 2 \\ \{(O_1, O_3)\}, & m = 3. \end{cases}$$

The different  $m$ -connectivity set  $N^{\mathcal{G}} \neq N^{\mathcal{G}'}$  indicates that  $\mathcal{G} = (O^{\mathcal{G}}, E^{\mathcal{G}})$  and  $\mathcal{G}' = (O^{\mathcal{G}'}, E^{\mathcal{G}'})$  are not equivalent and belong to the different causal relationship. Therefore, the  $m$ -connectivity property of node pairs can be used as a criterion for determining the equivalence of causal graphs.

Next, we explore the causal matrix space from the perspective of our sample mapping function  $\Phi(\mathbf{S}_{i,\cdot})$ . Specifically, we examine the design of equivalent square matrix that our sample mapping function maps to under certain conditions, laying the foundation for demonstrating that our mapping function can capture causal relationships. [10, 72, 30, 73] introduce the concept of the adjacency matrix, which represents the edge weights in a causal graph. [18] proposes using the adjacency matrix to guide network layers in capturing complex causal relationships between features. Inspired by [10, 18, 72, 30, 73], we introduce the notion of causal matrix to define equivalent condition for our sample mapping function  $\Phi(\mathbf{S}_{i,\cdot})$ . From the meaning behind Definition 4.2, it can be seen that the direction of our sample mapping function elements is crucial for determining the causal relationship between features. If the positive or negative signs of elements in two sets of samples match, it means the causal relationship between features is the same. Therefore, we construct a causal matrix to formalize the direction of our sample mapping function results  $\Phi(\mathbf{S}_{i,\cdot})$  and use it as an equivalent condition. In the causal matrix, we use 1 and -1 to represent the different directions: 1 for positive direction and -1 for negative direction.

**Definition 5.2 (Causal Matrix Space [10, 18, 72, 30, 73])** Consider  $m$ -order square matrix  $\mathbf{Y}$  and its causal matrix  $\text{sign}(\mathbf{Y}) \in \mathbb{R}^{m \times m}$  which is defined in (10). For two  $m$ -order square matrices  $\mathbf{Y}$  and  $\mathbf{Y}'$ , they are equivalent if and only if  $\text{sign}(\mathbf{Y}) = \text{sign}(\mathbf{Y}')$ . We use  $\mathbb{Y}^m$  to represent the space of equivalent causal matrices.

$$\text{sign}(\mathbf{Y})_{j,j'} = \begin{cases} 1, & \mathbf{Y}_{j,j'} \geq 0 \\ -1, & \mathbf{Y}_{j,j'} < 0 \end{cases}. \quad (13)$$

By defining the causal matrix and its space, we can formalize the potential causal relationship represented by our sample mapping function  $\Phi(\mathbf{S}_{i,\cdot})$ . We provide a simple example and mathematical proof to illustrate this.



*Proof.* Suppose the space of square matrix mapped by our sample mapping function  $\Phi(\mathbf{S}_{i,\cdot})$  is two-dimensional:  $\Phi(\mathbf{S}_{i,\cdot}) \in \mathbb{R}^{2 \times 2}$ . According to Definition 4.2 and Definition 5.2, for two square matrices mapped by our sample mapping function:  $\Phi(\mathbf{S}_{i,\cdot}) = \begin{bmatrix} a_{11} & a_{12} \\ a_{21} & a_{22} \end{bmatrix} = \begin{bmatrix} 0 & 0.8 \\ -0.2 & 0 \end{bmatrix}$ , and  $\Phi(\mathbf{S}_{i',\cdot}) = \begin{bmatrix} a'_{11} & a'_{12} \\ a'_{21} & a'_{22} \end{bmatrix} = \begin{bmatrix} 0 & 0.2 \\ -0.5 & 0 \end{bmatrix}$ , their respective causal matrices are denoted as:  $\text{sign}(\Phi(\mathbf{S}_{i,\cdot})) = \begin{bmatrix} 1 & 1 \\ -1 & 1 \end{bmatrix}$  and  $\text{sign}(\Phi(\mathbf{S}_{i',\cdot})) = \begin{bmatrix} 1 & 1 \\ -1 & 1 \end{bmatrix}$ . We find that  $\text{sign}(\Phi(\mathbf{S}_{i,\cdot}))$  and  $\text{sign}(\Phi(\mathbf{S}_{i',\cdot}))$  are the same. For the construction and meaning of our sample mapping function  $\Phi(\mathbf{S}_{i,\cdot})$ , the consistence of the element signs implies that the causal relationships underlying the features are consistent. Therefore, the causal matrix can serve as a criterion for determining the equivalence of square matrices. Meanwhile, it could reflect the underlying causal relationships captured by our mapping function.

Finally, we will explore the causal identifiability of our sample mapping function, ensuring that the method we proposed can identify heterogeneous subgroups and integrate with established causal learning methods for performance enhancement.

**Theorem 5.1** *The sample mapping function  $\Phi(\mathbf{S}_{i,\cdot})$  is an isomorphic mapping from the causal graph space  $\mathbb{Y}^m$  to the causal matrix space  $\mathbb{G}^m$ , thereby ensuring the isomorphism between the sample mapping space and the causal graph space.*

*Proof* [63, 64]. Consider two sample sets  $\mathbf{S} \in \mathbb{R}^{n \times m}$  and  $\mathbf{S}' \in \mathbb{R}^{n' \times m}$  with their respective causal graphs  $\mathcal{G}$  and  $\mathcal{G}'$ . Suppose the nonlinear causal relationships between them are equivalent, i.e.,  $N^{\mathcal{G}} = N^{\mathcal{G}'}$ . Let

$$\mathbf{I}_{j,j'} = \begin{cases} 1, & (j, j') \in N^{\mathcal{G}} \\ -1, & (j, j') \notin N^{\mathcal{G}} \end{cases} \quad (14)$$

Building upon Definition 4.3 and (13), our objective is to establish the equivalence of two causal matrices  $\text{sign}(\mathbf{Y})$  and  $\text{sign}(\mathbf{Y}')$ , generated by the sample mapping functions  $\Phi(\mathbf{S}_{i,\cdot})$  and  $\Phi(\mathbf{S}'_{i',\cdot})$ , respectively. Assuming the equivalence of causal matrices i.e.,  $\text{sign}(\mathbf{Y}) = \text{sign}(\mathbf{Y}')$ , for any pair  $(j, j') \in \{1, \dots, m\}$ , it can be demonstrated that  $\mathbf{Y}_{j,j'}$  and  $\mathbf{Y}'_{j,j'}$  share the same signs. Assuming  $\mathbf{Y}_{j,j'} > 0$  and  $\mathbf{Y}'_{j,j'} > 0$ , as per Definition 4.2, it is deducible that  $\Phi(\mathbf{S}_{i,\cdot})_{j,j'} > 0$  and  $\Phi(\mathbf{S}'_{i',\cdot})_{j,j'} > 0$ , leading to a similar conclusion from hypothesis testing. Referencing Theorem 4.1, this implies the presence of nonlinear dependence, i.e.,  $X_j \not\perp\!\!\!\perp X_{j'}$  in both sample sets  $\mathbf{S}$  and  $\mathbf{S}'$ , ensuring the equivalent of nonlinear causal relationships.

*Remark.* We provide an intuitive understanding for Theorem 5.1. For two causal graphs behind the data:  $\mathcal{G}$  and  $\mathcal{G}'$ , according to Definition 5.1, suppose they share the same pairs of nodes  $m$ -connectivity:  $N^{\mathcal{G}} = N^{\mathcal{G}'}$ . It implies that  $\mathcal{G}$  and  $\mathcal{G}'$  exhibit the same causal relationship:  $\mathcal{G} = \mathcal{G}'$ . Then, the matrix  $\mathbf{I}_{j,j'}$  can be constructed based on the  $m$ -connectivity set of node pair to represents the same meaning as (13) in Definition 5.2. Specifically, when node pair  $(j, j')$  belongs to this  $m$ -connectivity set, it indicates that there exists a causal relationship between nodes  $(j, j')$ , denoted as 1. Conversely, when node pair  $(j, j')$  does not belong to the  $m$ -connectivity set, it signifies the absence of the causal relationship, denoted as -1. For the square matrix mapped by our sample mapping function  $\Phi(\mathbf{S}_{i,\cdot})$ , if the corresponding matrix element is positive:  $\Phi(\mathbf{S}_{i,\cdot})_{j,j'} > 0$ , it indicates a causal relationship between the features  $X_j$  and  $X_{j'}$ :  $X_j \perp\!\!\!\perp X_{j'}$ . If the corresponding matrix element is negative:  $\Phi(\mathbf{S}_{i,\cdot})_{j,j'} < 0$ , it signifies no causal relationship between  $X_j$  and  $X_{j'}$ :  $X_j \not\perp\!\!\!\perp X_{j'}$ . Thus, in the causal graph space, if the node pair  $(j, j')$  belongs to our  $m$ -connectivity set, it is equivalent to the matrix element corresponding to features  $X_j$  and  $X_{j'}$  being positive. This ensures that our sample mapping function is consistent with the causal graph space in expressing causal relationships, demonstrating the causal identifiability of our sample mapping function.

These definitions and theorems contribute to a comprehensive understanding of the causal relationships revealed within the sample mapping function and its corresponding high-dimensional representation.

## 6 Experiments

In this section, experiments are conducted to validate our method from two perspectives. Both the generated synthetic data and real-world data sourced from the Indian Ocean Dipole [74] are employed to assess the accuracy of our method in identifying heterogeneous subgroups by identifying causal relationships between features. Furthermore, it is also proposed to deploy our method with popular causal learning methods to validate its effectiveness in enhancing causal learning using real-world Boston Housing Data from Kaggle.<sup>1</sup>

<sup>1</sup><https://www.kaggle.com/datasets/vikrishnan/boston-house-prices>.

## 6.1 Synthetic Data

*Baseline and Evaluation Metrics.* Various clustering methods are employed as benchmarks for performance comparison. K-means clustering (K-means) [75] with no kernel, chosen for its well-known partitional clustering, assigns distinct samples into  $k$  clusters based on proximity to cluster centers; polynomial kernel clustering (Poly) [76], known for modeling nonlinear relationships, maps samples into a higher-dimensional space to identify nonlinear boundaries between classes; radial basis function kernel clustering (RBF) [77], adept at clustering nonlinear separable samples, corresponds to an infinite-dimensional feature space, enabling complex decision boundaries. Both the V-measure Score (V-measure) and the Adjusted Rand Index (ARI) serve as metrics to evaluate the performance of these methods:

$$\text{V-measure} = \frac{2 \times H \times C}{H + C},$$

$$\text{ARI} = \frac{\text{RI} - \text{E}(\text{RI})}{\text{Max}(\text{RI}) - \text{E}(\text{RI})},$$

where  $H$  represents the homogeneity of the cluster,  $C$  represents the completeness of the cluster, and  $\text{RI}$  represents the Rand Index.

*Experimental setup.* Six random Directed Acyclic Graphs (DAGs) [78] are used to simulate heterogeneous subgroups, created with 10 variables  $X = (X_1, \dots, X_{10})$ , to model the causal relationships between them. In linear scenarios, random data with zero correlation ( $\text{corr} = 0$ ) between features is first generated by the process:

$$\mathbf{SD} = [SD_{X_1}, \dots, SD_{X_{10}}] \in \mathbb{R}^{100 \times 10},$$

denoted as

$$\mathbf{SD} = \sigma \cdot \mathbf{F} + \mu,$$

where  $\sigma$  follows a uniform distribution  $U(0.5, 2)$ ,  $\mathbf{F} \in \mathbb{R}^{100 \times 10}$  is a matrix with elements from a normal distribution  $N(0, 1)$ , and  $\mu \in \mathbb{R}^{100}$  is a column vector with elements from a uniform distribution  $U(-4, 4)$ . Subsequently, random data with non-zero correlation ( $\text{corr} \neq 0$ ) is generated by the following process:

$$SD_{X_p} = SD_{X_p} + \sum_{X_q \in \text{pa}(p)} w_{p,q} \cdot SD_{X_q},$$

where  $\text{pa}(p)$  represents the direct causal parent variables of  $X_p$ , and  $w_{p,q}$  represents the weight between  $X_p$  and  $X_q$ . In nonlinear scenarios, data are generated by adding randomized Gaussian noise.

Table 1: The clustering results of methods on both linear and nonlinear scenarios, where the higher V-measure and ARI denote better performances.

Methods	Linear								Nonlinear	
	$\text{corr} \neq 0, \mu \sim U(-4, 4)$		$\text{corr} \neq 0, \mu = 0$		$\text{corr} = 0, \mu \sim U(-4, 4)$		$\text{corr} = 0, \mu = 0$		V-measure	ARI
K-means [75]	0.59	0.53	0.52	0.35	0.55	0.38	0.51	0.31	0.07	0.14
Poly [76]	0.68	0.65	0.53	0.38	0.62	0.44	0.48	0.25	0.14	0.15
RBF [77]	0.65	0.59	0.56	0.47	0.61	0.42	0.14	0.21	0.26	0.15
<b>CKC (Ours)</b>	0.79	0.71	<b>0.65</b>	<b>0.56</b>	0.65	0.47	<b>0.59</b>	<b>0.43</b>	<b>0.40</b>	<b>0.23</b>

*Results.* As shown in TABLE 1, our method outperforms others in both linear and nonlinear scenarios. This highlights the capability of our method to handle data with causal relationships between features, even when the assumption of independence among features is relaxed. Furthermore, our method effectively addresses nonlinear causal relationships, indicating its broad applicability in real-world scenarios.

## 6.2 Real-world Data

In this section, the accuracy of our method in identifying heterogeneous subgroups is initially examined. Furthermore, our method is integrated into popular causal learning methods to assess the effectiveness of heterogeneous subgroup information in enhancing causal learning.

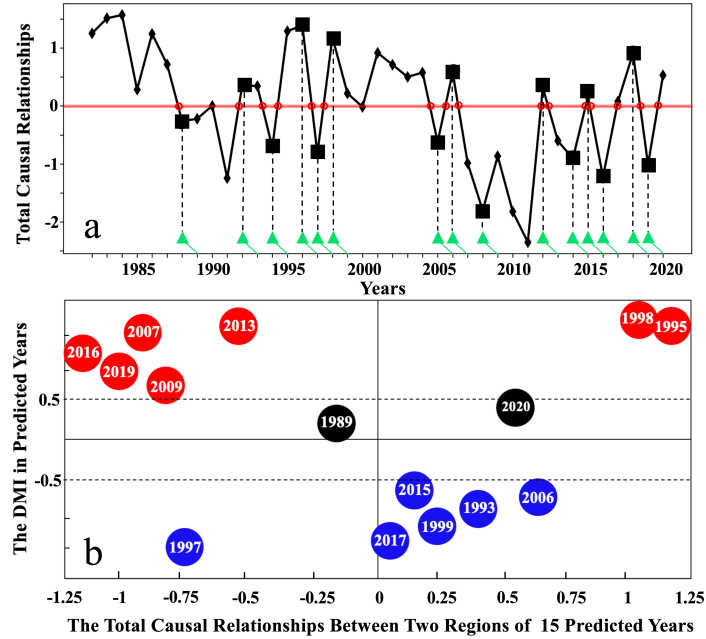


Figure 3: (a) The evolution of the standardized  $YC(y)$  time series. When it undergoes transitions (passing through red line) and reaches an extreme value (marked by black boxes), there is a possibility of an IOD event in the upcoming year (pointed with the green line). (b) The years predicted by our method are displayed in the circles. Both circles of blue and red represent IOD events among the correctly predicted. The black circles represent the wrongly predicted.

### 6.2.1 Experiments on Indian Ocean Dipole Data

The Indian Ocean Dipole (IOD) is a zonal dipole mode of the sea surface temperature (SST) that occurs interannually in the tropical Indian Ocean (TIO). Since IOD can affect the climate not only in the Indian Ocean rim countries but also in other more distant regions, it is of great importance to conduct IOD prediction [74]. With the causal structures... he cooperative behaviors among the grid points to detect possible TIO states that favor the development of the IOD.

*Baseline and Evaluation Metrics.* Three methods are used for comparisons for IOD warning: the CFSv2, ECs5, and the Network-based Approach (Net-based) [74]. The following metrics Accuracy, Recall, and F1-score are used as the metrics to illustrate the prediction accuracy, allowing for a comprehensive assessment of the ability to accurately identify IOD events:

$$\text{Accuracy} = \frac{TP+TN}{TP+TN+FP+FN},$$

$$\text{Recall} = \frac{TP}{TP+FN},$$

$$\text{F1-score} = \frac{2 \times TP}{FP+FN},$$

where TP represents true positive value, TN represents true negative value, FP represents false positive value, and FN represents false negative value.

*Experimental setup.* The public time-series data from [74] are employed for analyzing the Indian Ocean Dipole (IOD) event across two regions: the western region ( $10^{\circ}\text{N}$  to  $10^{\circ}\text{S}$ ,  $50^{\circ}\text{E}$  to  $70^{\circ}\text{E}$ ) and the eastern region ( $0$  to  $10^{\circ}\text{S}$ ,  $90^{\circ}\text{E}$  to  $110^{\circ}\text{E}$ ). The western region is partitioned into 441 grid nodes and the eastern region into 231 grid nodes, representing different areas. The analysis involves daily data spanning from 1982 to 2020, treating the nodes as features. To enable the classification of heterogeneous subgroups, the sample mapping function is devised, mapping the sample of each time point to a high-dimensional space.

The nonlinear causal kernel  $\kappa_{i,j}^t$  is constructed as the causal relationships between nodes by calculating the values of the sample mapping function at intersection times for each pair of nodes across the two regions, using a time point  $t$  of 60 days and a time lag parameter  $\theta$  set between 0 and 100 days:

$$\kappa_{i,j}^t(\theta) = \frac{\langle \Phi(T_i(t-\theta)), \Phi(T_j(t)) \rangle_{\text{F}}}{\|\Phi(T_i(t-\theta))\|_{\text{F}} \cdot \|\Phi(T_j(t))\|_{\text{F}}}, \quad (15)$$

$$\kappa_{i,j}^t(-\theta) = \frac{\langle \Phi(T_i(t)), \Phi(T_j(t-\theta)) \rangle_{\text{F}}}{\|\Phi(T_i(t))\|_{\text{F}} \cdot \|\Phi(T_j(t-\theta))\|_{\text{F}}}, \quad (16)$$

where  $\langle \cdot, \cdot \rangle_{\text{F}}$  represents the Frobenius inner product, and  $\|\cdot\|_{\text{F}}$  represents its norm, with  $i$  and  $j$  representing the nodes from regions of west (WE) and east (EA), respectively.

Table 2: The elements of the confusion matrices and the evaluation of methods mentioned in [74]. The direction of the arrow represents the direction in which the evaluation metrics are expected to vary.

Methods	True Positive ( $\uparrow$ )	True Negative ( $\uparrow$ )	False Positive ( $\downarrow$ )	False Negative ( $\downarrow$ )	Accuracy ( $\uparrow$ )	Recall ( $\uparrow$ )	F1-score ( $\uparrow$ )
CFSv2	4	16	11	5	0.56	0.44	0.33
ECs5	6	18	6	4	0.71	0.60	0.55
Net-based	11	16	4	6	0.73	0.65	0.69
<b>CKC (Ours)</b>	<b>13</b>	<b>22</b>	<b>2</b>	<b>2</b>	<b>0.90</b>	<b>0.87</b>	<b>0.87</b>

The total causal relationship  $\text{TC}(t)$  between the two regions at a given time point  $t$  is the sum of the causal relationships of all node pairs:

$$\text{TC}(t) = \sum_{i \in \text{WE}, j \in \text{EA}} \kappa_{i,j}^t(\theta) + \kappa_{i,j}^t(-\theta). \quad (17)$$

Since the causal relationships between regions differ between years with IOD events and normal years [79], the  $\text{YC}(y)$  is designed as the total causal relationships between two regions in a given year  $y$ , denoted as  $\text{YC}(y) = \sum_{t \in y} \text{TC}(t)$ ,  $y \in \{1982, \dots, 2020\}$ , allowing exploration of early causal warning signals.

*Results.* Fig. 3 (a) illustrates the evolution of the standardized  $\text{YC}(y)$  time series. We propose utilizing the time series  $\text{YC}(y)$  to cluster years into two subgroups, corresponding to years with IOD events and normal years. The results of clustering are determined based on the signs of  $\text{YC}(y)$ , indicating significantly different causal relationships between years with  $\text{YC}(y) > 0$  and  $\text{YC}(y) < 0$  (heterogeneous subgroups). Thus, it is inferred that when the sign of  $\text{YC}(y)$  undergoes a transition and  $\text{YC}(y)$  reaches an extreme value, the causal relationships between regions have probably varied. A fascinating finding is that an IOD event is more likely to occur in the following year due to these variations in causal relationships, serving as an early causal warning signal one year in advance. Fig. 3 (b) displays the predicted years with DMI [74], providing 15 warnings out of 15 IOD events, with 13 of these predictions being accurate. The ability of our method to identify heterogeneous subgroups and provide early causal warning is explicitly demonstrated. TABLE 2 shows the details of the confusion matrices and the evaluation metrics for the methods, highlighting the capacity of our method to predict more anomalous years while minimizing misleading predictions. This underscores the accuracy of our method in ensuring the reliability of identifying heterogeneous subgroups.

## 6.2.2 Experiments on Boston Housing Data

*Baseline and Evaluation Metrics.* Our method is deployed with popular causal learning methods to showcase the effectiveness of heterogeneous subgroup information in enhancing causal learning: ERM [19], for its broad applicability and effectiveness across diverse problem types; KerHRM [20], for its robustness to heterogeneity in data distributions; and Stable Learning [21, 22, 23], for its better performance in the presence of data distribution shifts between training and testing phases. The RMSE and the Sta\_Error are used as metrics to evaluate these enhancements:

$$\text{RMSE} = \sqrt{\frac{1}{n} \sum_{k=1}^n (Y_k - \hat{Y}_k)^2},$$

$$\text{Sta\_Error} = \text{RMSE}(D^{\text{test}}),$$

where  $n$  represents the number of samples,  $Y_k$  represents the true value of sample  $k$ ,  $\hat{Y}_k$  represent the predicted result for sample  $k$ , and  $D^{\text{test}}$  represents the test samples.

*Experimental setup.* The ability of the model to distinguish between causal and non-causal factors is essential, ensuring a focus on factors with causal relationships to the target. Our method achieves this by exploring the stability of relationships between features and the target using heterogeneous subgroup information. Features exhibiting higher stability of relationships are considered more likely to be causal factors. Subsequently, it is integrated with popular causal learning methods, prompting them to prioritize attention to these causal factors, thereby enhancing their generalizability.

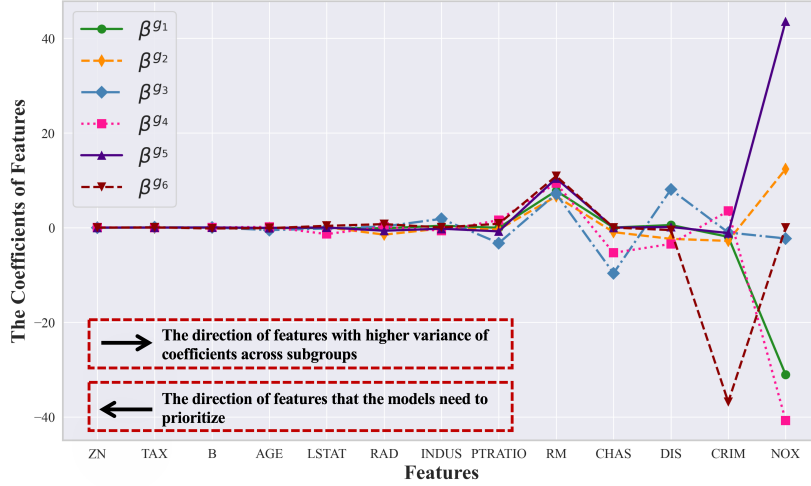


Figure 4: The coefficients  $\beta^{g_i}$  of features across heterogeneous subgroups  $G = \{g_1, g_2, \dots, g_6\}$  as learned by our method with  $K = 6$ . The features with lower variances of coefficients are more likely causal factors that the models need to prioritize.

For the heterogeneous subgroups identified by our method  $G = \{g_1, g_2, \dots, g_k\}$ , the regression coefficient  $\beta_p^{g_i}$  for each feature  $X_p$  within each identified subgroup  $g_i$  is first calculated, representing the relationship between  $X_p$  and target using traditional regression method:

$$Y^{g_i} = \beta_0^{g_i} + \beta_1^{g_i} X_1 + \dots + \beta_m^{g_i} X_m. \tag{18}$$

By aggregating the coefficients across different subgroups, each feature can be transformed into a vector space representing the combination of relationships under heterogeneous subgroups:

$$F(X_p) = (\beta_p^{g_1}, \beta_p^{g_2}, \dots, \beta_p^{g_k}). \tag{19}$$

The lower variance between the vector elements for the feature indicates a more stable relationship with the target. Thus, the feature is more likely a causal factor that the models need to prioritize.

Table 3: The results of our method after deploying to popular causal learning methods across various cluster scenarios  $K = \{2, 3, 4, 5, 6\}$ , where the best results are denoted as bolded. Our method is robust to the selection of parameter  $K$ , reducing the predicted error in almost all scenarios (underlines).

Methods	ERM [19]		KerHRM [20]		DWR [21]		SRDO [22]		SVI [23]	
	RMSE	Sta_Error	RMSE	Sta_Error	RMSE	Sta_Error	RMSE	Sta_Error	RMSE	Sta_Error
Cluster Scenarios	3.09	24.68	21.43	23.43	0.80	26.57	0.22	19.11	0.41	15.30
+CKC(K=2)	4.70	<b>8.60</b>	18.92	<u>11.41</u>	1.96	<b>13.46</b>	0.48	<u>7.68</u>	0.56	<b>12.75</b>
+CKC(K=3)	3.29	<u>8.83</u>	12.31	<b>10.54</b>	1.56	<u>14.30</u>	0.23	<u>8.60</u>	0.45	<u>12.99</u>
+CKC(K=4)	4.69	<u>12.23</u>	24.03	<u>12.01</u>	1.95	<u>19.46</u>	0.67	<u>13.92</u>	0.45	<u>13.63</u>
+CKC(K=5)	4.68	<u>12.39</u>	10.92	<u>13.86</u>	1.92	<u>26.11</u>	0.44	<b>6.88</b>	0.44	<u>13.35</u>
+CKC(K=6)	3.29	<u>8.82</u>	22.26	<u>11.78</u>	1.54	<u>20.39</u>	0.25	<u>9.07</u>	0.45	<u>13.25</u>

*Results.* Fig. 4 displays the coefficients of features under different subgroups  $G = \{g_1, g_2, \dots, g_6\}$  as learned by our method with  $K = 6$ . This choice of  $K$  facilitates a clearer and more distinct presentation of the results. Our method effectively utilizes heterogeneous subgroups to identify the causal factors, directing models to prioritize them. Table 3 outlines the outcomes of deploying our method to popular causal learning methods across diverse cluster scenarios  $K = \{2, 3, 4, 5, 6\}$ , demonstrating the effectiveness of our method in enhancing causal learning. An important observation is the robustness of our method across varying cluster scenarios  $K$ . This suggests that determining the precise number of heterogeneous subgroups in advance is not crucial, as long as it accurately captures the heterogeneous subgroup information. The flexibility embedded in our method enhances its generalizability, enabling adaptation to various scenarios without compromising its effectiveness in capturing heterogeneous subgroups.

## 7 Conclusion

The central challenge we address pertains to the problem of heterogeneous subgroup causal learning arising from multi-source and heterogeneous data. This issue stems from the limitations of a single causal model in adequately capturing variations in causal relationships. In this paper, a novel method is proposed for heterogeneous subgroup causal learning through the nonlinear Causal Kernel Clustering (CKC) method. Diverging from conventional methods that apply a single causal model to the entire data set, often resulting in insufficient representation and overlooking data diversity nuances, our method introduces a sample mapping function and a corresponding nonlinear causal kernel for clustering. This ensures that samples within each cluster exhibit more closely aligned causal relationships. Serving as a flexible causal discovery module, our method not only addresses heterogeneous subgroups across different data types but also enhances causal learning. Its remarkable generalizability positions it as a valuable tool for various applications characterized by the prevalence of multi-source and heterogeneous data.

## Acknowledgments

## References

- [1] Clark Glymour, Kun Zhang, and Peter Spirtes. Review of Causal Discovery Methods Based on Graphical Models. *Frontiers in Genetics*, 10, 2019.
- [2] Bernhard Schölkopf, Francesco Locatello, Stefan Bauer, Nan Rosemary Ke, Nal Kalchbrenner, Anirudh Goyal, and Yoshua Bengio. Toward Causal Representation Learning. *Proceedings of the IEEE*, 109(5):612–634, 2021.
- [3] Yunxia Wang, Fuyuan Cao, Kui Yu, and Jiye Liang. Local Causal Discovery in Multiple Manipulated Datasets. *IEEE Transactions on Neural Networks and Learning Systems*, 34(10):7235–7247, 2023.
- [4] Ruocheng Guo, Lu Cheng, Jundong Li, P. Richard Hahn, and Huan Liu. A Survey of Learning Causality with Data: Problems and Methods. *ACM Comput. Surv.*, 53(4), jul 2020.
- [5] Alex Markham, Danai Deligeorgaki, Pratik Misra, and Liam Solus. A Transformational Characterization of Unconditionally Equivalent Bayesian Networks. In *Proceedings of The 11th International Conference on Probabilistic Graphical Models*, pages 109–120. PMLR, 2022.
- [6] Alex Markham and Moritz Grosse-Wentrup. Measurement Dependence Inducing Latent Causal Models. In *Proceedings of the 36th Conference on Uncertainty in Artificial Intelligence (UAI)*, pages 590–599. PMLR, 2020.
- [7] Biwei Huang, Kun Zhang, Jiji Zhang, Joseph Ramsey, Ruben Sanchez-Romero, Clark Glymour, and Bernhard Schölkopf. Causal Discovery from Heterogeneous/Nonstationary Data. *Journal of Machine Learning Research*, 21(89):1–53, 2020.
- [8] Vaishali Mahipal and Mohammad Arif Ul Alam. Estimating Heterogeneous Causal Effect of Polysubstance Usage on Drug Overdose from Large-Scale Electronic Health Record. In *2022 44th Annual International Conference of the IEEE Engineering in Medicine & Biology Society (EMBC)*, pages 1028–1031, 2022.
- [9] Hao Zhou, Shaoming Li, Guibin Jiang, Jiaqi Zheng, and Dong Wang. Direct Heterogeneous Causal Learning for Resource Allocation Problems in Marketing. *Proceedings of the AAAI Conference on Artificial Intelligence*, 37(4):5446–5454, Jun. 2023.
- [10] Yuhao Wang, Santiago Segarra, and Caroline Uhler. High-dimensional joint estimation of multiple directed Gaussian graphical models. *Electronic Journal of Statistics*, 14(1):2439 – 2483, 2020.
- [11] Kun Zhang and Madelyn RK Glymour. Unmixing for causal inference: Thoughts on mcaffrey and danks. *The British Journal for the Philosophy of Science*, 2020.
- [12] Sindy Löwe, David Madras, Richard Zemel, and Max Welling. Amortized Causal Discovery: Learning to Infer Causal Graphs from Time-Series Data. In Bernhard Schölkopf, Caroline Uhler, and Kun Zhang, editors, *Proceedings of the First Conference on Causal Learning and Reasoning*, volume 177 of *Proceedings of Machine Learning Research*, pages 509–525. PMLR, 11–13 Apr 2022.
- [13] Chenxi Liu and Kun Kuang. Causal Structure Learning for Latent Intervened Non-stationary Data. In Andreas Krause, Emma Brunskill, Kyunghyun Cho, Barbara Engelhardt, Sivan Sabato, and Jonathan Scarlett, editors, *Proceedings of the 40th International Conference on Machine Learning*, volume 202 of *Proceedings of Machine Learning Research*, pages 21756–21777. PMLR, 23–29 Jul 2023.
- [14] Hong Chen, Yingjie Wang, Feng Zheng, Cheng Deng, and Heng Huang. Sparse Modal Additive Model. *IEEE Transactions on Neural Networks and Learning Systems*, 32(6):2373–2387, 2021.

- [15] Shoubo Hu, Zhitang Chen, Vahid Partovi Nia, Laiwan CHAN, and Yanhui Geng. Causal Inference and Mechanism Clustering of A Mixture of Additive Noise Models. In S. Bengio, H. Wallach, H. Larochelle, K. Grauman, N. Cesa-Bianchi, and R. Garnett, editors, *Advances in Neural Information Processing Systems*, volume 31. Curran Associates, Inc., 2018.
- [16] Xingyu Wu, Bingbing Jiang, Yan Zhong, and Huanhuan Chen. Multi-label causal variable discovery: Learning common causal variables and label-specific causal variables. *arXiv preprint arXiv:2011.04176*, 2020.
- [17] Abdellah Rahmani and Pascal Frossard. Causal Temporal Regime Structure Learning. *arXiv preprint arXiv:2311.01412*, 2024.
- [18] Matthew J. Vowels, Necati Cihan Camgoz, and Richard Bowden. D’ya Like DAGs? A Survey on Structure Learning and Causal Discovery. *ACM Comput. Surv.*, 55(4), November 2022.
- [19] V. Vapnik. Principles of Risk Minimization for Learning Theory. In J. Moody, S. Hanson, and R.P. Lippmann, editors, *Advances in Neural Information Processing Systems*, volume 4. Morgan-Kaufmann, 1991.
- [20] Jiashuo Liu, Zheyuan Hu, Peng Cui, Bo Li, and Zheyuan Shen. Integrated Latent Heterogeneity and Invariance Learning in Kernel Space. In M. Ranzato, A. Beygelzimer, Y. Dauphin, P.S. Liang, and J. Wortman Vaughan, editors, *Advances in Neural Information Processing Systems*, volume 34, pages 21720–21731. Curran Associates, Inc., 2021.
- [21] Kun Kuang, Ruoxuan Xiong, Peng Cui, Susan Athey, and Bo Li. Stable Prediction with Model Misspecification and Agnostic Distribution Shift. *Proceedings of the AAAI Conference on Artificial Intelligence*, 34(04):4485–4492, Apr. 2020.
- [22] Zheyuan Shen, Peng Cui, Tong Zhang, and Kun Kunag. Stable Learning via Sample Reweighting. *Proceedings of the AAAI Conference on Artificial Intelligence*, 34(04):5692–5699, Apr. 2020.
- [23] Han Yu, Peng Cui, Yue He, Zheyuan Shen, Yong Lin, Renzhe Xu, and Xingxuan Zhang. Stable Learning via Sparse Variable Independence. *Proceedings of the AAAI Conference on Artificial Intelligence*, 37(9):10998–11006, Jun. 2023.
- [24] Georgios Mavroudeas, Nafis Neehal, Jason Kuruzovich, Kristin P. Bennett, and Malik Magdon-Ismael. Sub-population Analysis in Causal Inference: A Healthcare Case Study. In *2022 IEEE International Conference on Bioinformatics and Biomedicine (BIBM)*, pages 1673–1676, 2022.
- [25] Wei Chen, Yunjin Wu, Ruichu Cai, Yueguo Chen, and Zhifeng Hao. CCSL: a causal structure learning method from multiple unknown environments. *arXiv preprint arXiv:2111.09666*, 2021.
- [26] Elias Bareinboim and Judea Pearl. Causal inference and the data-fusion problem. *Proceedings of the National Academy of Sciences*, 113(27):7345–7352, 2016.
- [27] Ankit Sharma, Garima Gupta, Ranjitha Prasad, Arnab Chatterjee, Lovekesh Vig, and Gautam Shroff. MetaCI: Meta-learning for causal inference in a heterogeneous population. *arXiv preprint arXiv:1912.03960*, 2019.
- [28] Ahmed M. Alaa and Mihaela van der Schaar. Bayesian Inference of Individualized Treatment Effects using Multi-task Gaussian Processes. In I. Guyon, U. Von Luxburg, S. Bengio, H. Wallach, R. Fergus, S. Vishwanathan, and R. Garnett, editors, *Advances in Neural Information Processing Systems*, volume 30. Curran Associates, Inc., 2017.
- [29] Alex Markham, Richeek Das, and Moritz Grosse-Wentrup. A Distance Covariance-based Kernel for Nonlinear Causal Clustering in Heterogeneous Populations. In Bernhard Schölkopf, Caroline Uhler, and Kun Zhang, editors, *Proceedings of the First Conference on Causal Learning and Reasoning*, volume 177 of *Proceedings of Machine Learning Research*, pages 542–558. PMLR, 11–13 Apr 2022.
- [30] Ignavier Ng, Shengyu Zhu, Zhuangyan Fang, Haoyang Li, Zhitang Chen, and Jun Wang. Masked gradient-based causal structure learning. In *Proceedings of the 2022 SIAM International Conference on Data Mining (SDM)*, pages 424–432. SIAM, 2022.
- [31] Shengyu Zhu, Ignavier Ng, and Zhitang Chen. Causal Discovery with Reinforcement Learning. *arXiv preprint arXiv:1906.04477*, 2019.
- [32] Dag Tjøstheim, Håkon Otneim, and Bård Støve. Statistical Dependence: Beyond Pearson’s  $\rho$ . *Statistical Science*, 37(1):90–109, 2022.
- [33] Shun Yao, Xianyang Zhang, and Xiaofeng Shao. Testing Mutual Independence in High Dimension via Distance Covariance. *Journal of the Royal Statistical Society Series B: Statistical Methodology*, 80(3):455–480, 10 2017.
- [34] Arthur Gretton, Kenji Fukumizu, and Bharath K Sriperumbudur. Discussion of: Brownian distance covariance. *The annals of applied statistics*, 3(4):1285–1294, 2009.

- [35] Gábor J. Székely and Maria L. Rizzo. Partial distance correlation with methods for dissimilarities. *The Annals of Statistics*, 42(6):2382 – 2412, 2014.
- [36] Mary L McHugh. The Chi-square test of independence. *Biochemia Medica*, 23(2):143–149, 2013.
- [37] Eric Benhamou and Valentin Melot. Seven proofs of the Pearson Chi-squared independence test and its graphical interpretation. *arXiv preprint arXiv:1808.09171*, 2018.
- [38] Shubhadeep Chakraborty and Xianyang Zhang. A new framework for distance and kernel-based metrics in high dimensions. *Electronic Journal of Statistics*, 15(2):5455 – 5522, 2021.
- [39] Themistoklis Koutsellis, Stylianos Choumas, Alexandros Nikas, Christopher Ververidis, Thomas Papapolyzos, Anastasios Bitsikas, Ioanna Makarouni, and Haris Doukas. Serial Dependence Analysis of Time Series Using Distance Correlation and Monte Carlo Bootstrap Hypothesis Test. In *2023 14th International Conference on Information, Intelligence, Systems & Applications (IISA)*, pages 1–8, 2023.
- [40] Kashif Yousuf and Yang Feng. Targeting Predictors Via Partial Distance Correlation With Applications to Financial Forecasting. *Journal of Business & Economic Statistics*, 40(3):1007–1019, 2022.
- [41] Sambit Panda Cencheng Shen and Joshua T. Vogelstein. The Chi-Square Test of Distance Correlation. *Journal of Computational and Graphical Statistics*, 31(1):254–262, 2022. PMID: 35707063.
- [42] A. Sayago A. G. Asuero and A. G. González. The Correlation Coefficient: An Overview. *Critical Reviews in Analytical Chemistry*, 36(1):41–59, 2006.
- [43] Khawla Ali Abd Al-Hameed. Spearman’s correlation coefficient in statistical analysis. *International Journal of Nonlinear Analysis and Applications*, 13(1):3249–3255, 2022.
- [44] Hongfang Zhou, Xiqian Wang, and Rourou Zhu. Feature selection based on mutual information with correlation coefficient. *Applied intelligence*, 52(5):5457–5474, 2022.
- [45] Ting Wang and Shiqiang Zhang. Study on linear correlation coefficient and nonlinear correlation coefficient in mathematical statistics. *Studies in Mathematical Sciences*, 3(1):58–63, 2011.
- [46] Changbo Zhu, Xianyang Zhang, Shun Yao, and Xiaofeng Shao. Distance-based and RKHS-based dependence metrics in high dimension. *The Annals of Statistics*, 48(6):3366–3394, 2020.
- [47] Feng Xie, Biwei Huang, Zhengming Chen, Yangbo He, Zhi Geng, and Kun Zhang. Identification of Linear Non-Gaussian Latent Hierarchical Structure. In Kamalika Chaudhuri, Stefanie Jegelka, Le Song, Csaba Szepesvari, Gang Niu, and Sivan Sabato, editors, *Proceedings of the 39th International Conference on Machine Learning*, volume 162 of *Proceedings of Machine Learning Research*, pages 24370–24387. PMLR, 17–23 Jul 2022.
- [48] Chandler Squires, Annie Yun, Eshaan Nichani, Raj Agrawal, and Caroline Uhler. Causal Structure Discovery between Clusters of Nodes Induced by Latent Factors. In Bernhard Schölkopf, Caroline Uhler, and Kun Zhang, editors, *Proceedings of the First Conference on Causal Learning and Reasoning*, volume 177 of *Proceedings of Machine Learning Research*, pages 669–687. PMLR, 11–13 Apr 2022.
- [49] Jeffrey Adams, Niels Hansen, and Kun Zhang. Identification of Partially Observed Linear Causal Models: Graphical Conditions for the Non-Gaussian and Heterogeneous Cases. In M. Ranzato, A. Beygelzimer, Y. Dauphin, P.S. Liang, and J. Wortman Vaughan, editors, *Advances in Neural Information Processing Systems*, volume 34, pages 22822–22833. Curran Associates, Inc., 2021.
- [50] Amy Nowacki. Chi-square and Fisher’s exact tests. *Cleve Clin J Med*, 84(9 suppl 2):e20–5, 2017.
- [51] Weddha Savitri, Ni Luh Sutjiati Beratha, I Nengah Sudipa, and I Made Rajeg. Applying Chi-Square Test In Measuring The Significance Of The Occurrence Of French Synonym In Corpus Data. *International Journal of Linguistics and Discourse Analytics*, 6(1):13–21, 2024.
- [52] Christopher N Foley, Amy M Mason, Paul D W Kirk, and Stephen Burgess. MR-Clust: clustering of genetic variants in Mendelian randomization with similar causal estimates. *Bioinformatics*, 37(4):531–541, 09 2020.
- [53] Fateme Nateghi Haredasht, Farnaz Ghassemi, and Mohammad Hassan Moradi. Causal inference of gene expression data using a clustering-based extension of Kernel-Granger causality. In *2016 23rd Iranian Conference on Biomedical Engineering and 2016 1st International Iranian Conference on Biomedical Engineering (ICBME)*, pages 84–88, 2016.
- [54] Xingxuan Zhang, Peng Cui, Renzhe Xu, Linjun Zhou, Yue He, and Zheyang Shen. Deep Stable Learning for Out-of-Distribution Generalization. In *Proceedings of the IEEE/CVF Conference on Computer Vision and Pattern Recognition (CVPR)*, pages 5372–5382, June 2021.
- [55] Jiakuan Liang, Jun Wang, Guoxian Yu, Shuyin Xia, and Guoyin Wang. Multi-Granularity Causal Structure Learning. *Proceedings of the AAAI Conference on Artificial Intelligence*, 38(12):13727–13735, Mar. 2024.



- [56] Jianhong Chen, Ying Ma, and Xubo Yue. Temporal Causal Discovery in Dynamic Bayesian Networks Using Federated Learning. *arXiv preprint arXiv:2412.09814*, 2024.
- [57] Peng Tang, Guoru Ding, Yitao Xu, Yutao Jiao, Yehui Song, and Guofeng Wei. Causal Learning for Robust Specific Emitter Identification Over Unknown Channel Statistics. *IEEE Transactions on Information Forensics and Security*, 19:5316–5329, 2024.
- [58] Hidehiro Kato, Yasuyuki Nogami, Tomoki Yoshida, and Yoshitaka Morikawa. Cyclic vector multiplication algorithm based on a special class of gauss period normal basis. *ETRI journal*, 29(6):769–778, 2007.
- [59] Angelika Rohde and Alexandre B. Tsybakov. Estimation of high-dimensional low-rank matrices. *The Annals of Statistics*, 39(2):887 – 930, 2011.
- [60] Xi Luo. High Dimensional Low Rank and Sparse Covariance Matrix Estimation via Convex Minimization. *arXiv preprint arXiv:1111.1133*, 2011.
- [61] Ronald Katende. Efficient Matrix Decomposition for High-Dimensional Structured Systems: Theory and Applications. *arXiv preprint arXiv:2409.06321*, 2024.
- [62] Pei-Chang Guo. A Frobenius Norm Regularization Method for Convolutional Kernel Tensors in Neural Networks. *Computational Intelligence and Neuroscience*, 2022(1):3277730, 2022.
- [63] Thomas W Judson. *Abstract algebra: theory and applications*. 2020.
- [64] Sandhya S Pai and Thankanchan Baiju. Continuous mappings in soft lattice topological spaces. *Italian J. Pure Appl. Math.(Communicated)*, 2022.
- [65] Kacper Pluta, Pascal Romon, Yukiko Kenmochi, and Nicolas Passat. Bijective digitized rigid motions on subsets of the plane. *Journal of Mathematical Imaging and Vision*, 59:84–105, 2017.
- [66] Jiří Fiala and Jan Kratochvíl. Locally constrained graph homomorphisms—structure, complexity, and applications. *Computer Science Review*, 2(2):97–111, 2008.
- [67] Xiaorui Sun. Faster Isomorphism for  $p$ -Groups of Class 2 and Exponent  $p$ . In *Proceedings of the 55th Annual ACM Symposium on Theory of Computing, STOC 2023*, page 433–440, New York, NY, USA, 2023. Association for Computing Machinery.
- [68] Sander Beckers. Equivalent causal models. In *Proceedings of the AAAI Conference on Artificial Intelligence*, volume 35, pages 6202–6209, 2021.
- [69] Murat Kocaoglu. Characterization and Learning of Causal Graphs with Small Conditioning Sets. In A. Oh, T. Naumann, A. Globerson, K. Saenko, M. Hardt, and S. Levine, editors, *Advances in Neural Information Processing Systems*, volume 36, pages 74140–74179. Curran Associates, Inc., 2023.
- [70] Jun Otsuka and Hayato Saigo. On the equivalence of causal models: A category-theoretic approach. In *Conference on Causal Learning and Reasoning*, pages 634–646. PMLR, 2022.
- [71] Paul K Rubenstein, Sebastian Weichwald, Stephan Bongers, Joris M Mooij, Dominik Janzing, Moritz Grosse-Wentrup, and Bernhard Schölkopf. Causal Consistency of Structural Equation Models. *arXiv preprint arXiv:1707.00819*, 2017.
- [72] Zhaobin Mo, Qingyuan Liu, Baohua Yan, Longxiang Zhang, and Xuan Di. Causal Adjacency Learning for Spatiotemporal Prediction Over Graphs. *arXiv preprint arXiv:2411.16142*, 2024.
- [73] Zhuangyan Fang, Shengyu Zhu, Jiji Zhang, Yue Liu, Zhitang Chen, and Yangbo He. On low-rank directed acyclic graphs and causal structure learning. *IEEE Transactions on Neural Networks and Learning Systems*, 35(4):4924–4937, 2023.
- [74] Zhenghui Lu, Wenjie Dong, Bo Lu, Naiming Yuan, Zhuguo Ma, Mikhail I. Bogachev, and Juergen Kurths. Early warning of the Indian Ocean Dipole using climate network analysis. *Proceedings of the National Academy of Sciences*, 119(11):e2109089119, 2022.
- [75] Kristina P. Sinaga and Miin-Shen Yang. Unsupervised K-Means Clustering Algorithm. *IEEE Access*, 8:80716–80727, 2020.
- [76] Vahid Hooshmand Moghaddam and Javad Hamidzadeh. New Hermite orthogonal polynomial kernel and combined kernels in Support Vector Machine classifier. *Pattern Recognition*, 60:921–935, 2016.
- [77] Zuzana Majdisova and Vaclav Skala. Radial basis function approximations: comparison and applications. *Applied Mathematical Modelling*, 51:728–743, 2017.
- [78] Ari M. Lipsky and Sander Greenland. Causal Directed Acyclic Graphs. *JAMA*, 327(11):1083–1084, 03 2022.

- [79] G. Di Capua, J. Runge, R. V. Donner, B. van den Hurk, A. G. Turner, R. Vellore, R. Krishnan, and D. Coumou. Dominant patterns of interaction between the tropics and mid-latitudes in boreal summer: causal relationships and the role of timescales. *Weather and Climate Dynamics*, 1(2):519–539, 2020.